Applied Catalysis B: Environmental 224 (2018) 376–382

Contents lists available at ScienceDirect

Applied Catalysis B: Environmental

journal homepage: www.elsevier.com/locate/apcatb

Research Paper

Enhancement of photocatalytic decarboxylation on TiO_2 by water-induced change in adsorption-mode

Hongna Zhang[a,b], Peng Zhou[a,b], Hongwei Ji[a], Wanhong Ma[a], Chuncheng Chen[a,*], Jincai Zhao[a]

[a] Key Laboratory of Photochemistry, CAS Research/Education Center for Excellence in Molecular Sciences, Institute of Chemistry, Chinese Academy of Sciences, Beijing, 100190, PR China

[b] University of Chinese Academy of Sciences, Beijing, 100049, PR China

ARTICLE INFO

Keywords:
Photocatalytic decarboxylation
Acetic acid
Adsorption mode
Gas-solid interface
Titanium dioxide

ABSTRACT

Decarboxylation is an important process in the photocatalytic degradation of organic pollutants. In this study, the adsorption and photocatalytic decarboxylation of acetic acid and trichloroacetic acid were investigated by in-situ diffuse reflectance Fourier transform infrared spectroscopy (DRIFTS), which can distinguish carboxylate groups with different adsorption modes. We found that water molecules promote photocatalytic decarboxylation reaction and the promotional effect of water is attributed to the changed adsorption mode of the carboxylate group by the co-adsorbed water molecules. The IR study shows that degradation of the monodentate-coordinated acetic acids is much faster than that of the bidentate-coordinated one. The kinetic isotope effect studies and analysis of the intermediate products indicates that the degradation of acetic acids originates from the direct oxidation by holes even in the presence of water, rather than from the reaction of OH radicals as generally believed. DFT-based molecular dynamics calculations revealed that the formation of the monodentate-coordinated carboxylate group in the presence of water is attributed to competition between the O atom of the carboxylate group and water for the surface Ti sites. Because of its higher electron density, the monodentate carboxylate group is easier to be directly oxidized by holes than the bidentate group.

1. Introduction

TiO_2 photocatalysis has been widely used to degrade organic pollutants in water [1–6] and air [7–9], to clean the surface of glass and buildings [10–12] and to accelerate the transformation of atmospheric organic compounds [4,13]. During these degradation reactions, stable carboxylic intermediates are usually accumulated on the surface of the photocatalyst before the organic substrates are completely mineralized to CO_2 [14–19]. The strong adsorption ability of these carboxylic intermediates on the TiO_2 surface hinders interactions between the surface and other organic pollutants, which consequently decreases the photoactivity of the photocatalyst for sustained reactions. Therefore, photocatalytic decarboxylation is an important process for the photocatalytic degradation of organic pollutants.

Water molecules are ubiquitous in photocatalytic systems and are known to markedly influence the photocatalytic rate and pathway [1,14,17,19]. For example, for the photocatalytic oxidation of ethanol, the presence of water vapor depresses largely the degradation reactions [17]. The depressive effect has been attributed to the competition of water molecules for the surface sites of the photocatalyst, which hinders the interaction of ethanol with the surface. However, water vapor (humidity) has been reported to enhance the photocatalytic degradation of carboxylic acids, such as formic acid [20,21] and acetic acid [17,22]. Because the adsorption of carboxylic acids on TiO_2 is much stronger than that water molecules [23], the enhancement effect of water is usually explained by the increased yield of OH radicals in the presence of water [17,22,24] or by the more facile desorption of the degradation product [14,25]. The influence of water on the photocatalytic degradation of carboxylic acid never is considered from the aspect of the interaction change. Actually, the presence of water molecules has been shown to affect the adsorption mode of carboxylic compounds on TiO_2. For example, the theoretical calculation showed that the addition of water promotes O—H bond dissociation of formic acid to produce formate ions [26]. The recently experiment results also suggested that under low humility to yield formic acid adsorbed as bridged bidentate formate and under higher humility as molecularly adsorbed formic acid [27]. However, the relationship between the change of the adsorption mode on TiO_2 and the enhancement effect of the water on the photocatalytic degradation of carboxylic compounds is largely missed.

* Corresponding author.
E-mail address: ccchen@iccas.ac.cn (C. Chen).

http://dx.doi.org/10.1016/j.apcatb.2017.10.020
Received 11 July 2017; Received in revised form 28 September 2017; Accepted 9 October 2017
Available online 10 October 2017

In the present work, we study the effect of co-adsorbed water molecules on the adsorption and photocatalytic decarboxylation of carboxylic compounds on the gas-solid interface of TiO_2 via in-situ diffuse reflectance infrared spectroscopy, kinetic isotope effect studies, gas chromatography–mass spectroscopy (GC/MS), gas chromatography (GC), and theoretical calculations. Acetic acid and trichloroacetic acid (TCA) were used as model carboxylic compounds. Our experiments suggest that the enhancement effects of water vapor on the degradation of carboxylic acids originates dominantly from the changed adsorption mode of the carboxylate, rather than from the enhanced yield of OH radicals as generally believed. The mechanism underlying the experimental observations was also discussed on the base of the DFT calculations. The present study implies that the adsorption mode of carboxylic acids on TiO_2 would largely influence the interfacial charge transfer process during the photocatalytic reaction.

2. Experimental

2.1. DRIFTS measurements

A Thermo Nicolet 6700 Fourier transform infrared (FTIR) spectrometer equipped with a mercury cadmium telluride (MCT) detector was used for the diffuse reflectance FTIR measurements (DRIFTS). A praying mantis diffuse reflectance accessory and a reaction cell equipped with a heater (Harrick Scientific) were employed for the in situ sample treatment, photocatalytic reaction and IR detection, as described in our previous report [28]. 100 mg of TiO_2 samples were housed at a sample cup inside the reaction cell. The cell was covered with a dome containing three windows: two were made of ZnSe to permit the entry and exit of the infrared beam, and the third (quartz) was for the transmission of the UV-light beam. Before the IR measurement, the samples were heated at 723 K for 1 h under O_2 flow (50 mL min^{-1}) to remove water molecules and organic residues and to heal any O-vacancies existing on the surface. The samples were subsequently cooled to 298 K under O_2 flow. The above process is called the dehydration process in the following discussion. Acetic acid was introduced onto the TiO_2 surface by the on-line flow of O_2 (50 mL min^{-1}) from a glass bottle with a given amount of acetic acid vapor. H_2O or D_2O was introduced by flushing with O_2-saturated liquid H_2O or D_2O at 303 K, and their amount on TiO_2 was controlled by heating the samples at a given temperature. All the IR measurements were carried out at 303 K under O_2 atmosphere. For the adsorption and oxidation of TCA, TCA was pre-adsorbed on TiO_2 by soaking the sample in a 0.5 mM TCA solution. After centrifugation, the samples were dried at 453 K for 12 h. UV irradiation was performed with a 365 nm LED (5 W). IR spectra ranging from 4000 to 1000 cm^{-1} with a resolution of 4 cm^{-1} were recorded by averaging 32 scans. Absorbance units, which were used specifically for the reflectance spectra, were used to measure the spectral intensity.

2.2. Intermediate analysis

Identification of the products after the photocatalytic oxidation of acetic acid was achieved using a GC/MS (Agilent 7890A/5975C) system equipped with a HP-5MS column (30 m × 0.25 mm × 0.25 μm). The GC/MS features were identified by comparing the mass fragmentation patterns of the products with patterns from the built-in Wiley/NIST library. Quantitative analysis of the intermediates formed during the photocatalytic oxidation of acetic acid was achieved using a GC (Agilent 7890A), equipped with a DM-5 Amine column (30 m × 0.25 mm × 0.50 μm) and a flame ionization detector. Identification of the GC features was confirmed using authentic compounds.

2.3. Theoretic calculations

The Vienna Ab initio Simulation Package (VASP) was used for the DFT-based molecular dynamics calculations [29–32]. It is well known that the (101) surface is the most stable and therefore the most abundant surface in anatase, which was used in our study. The strong {101} diffraction peak in our XRD results (Fig. S1) also confirm that the used TiO_2 mainly exposes the {101} facet. Accordingly, the DFT calculations were carried out on the {101} surface, by a repeating 1 × 3 supercell model with 6 O—Ti—O layers. In the initial model, a water molecules is located on the TiO_2 {101} surfaces by constructing a Ti—O bond between the O atom of adsorbed H_2O and the surface Ti atom. The CH_3COOH molecule was adsorbed on the TiO_2 {101} surface by the dissociative mode. One H atom from the CH_3COOH molecule was adsorbed at one bridge O atom of TiO_2, while the left CH_3COO group was located on the TiO_2 {101} surface by two modes. In the first mode, the left CH_3COO group is adjacent to the adsorbed H_2O. In the second mode, the left CH_3COO group is far away from the adsorbed H_2O. Interactions between the adjacent atom slabs were eliminated by including a 20 Å-thick vacuum slab. The generalized gradient approximation (GGA) of Perdew–Burke–Ernzerhof (PBE) was used as the exchange-correlation functional [33,34]. The interaction between valence electrons and the ionic core was described by the PAW pseudopotential. A cutoff energy of 450 eV and a Monkhorst-Pack k-point mesh of 4 × 4 × 1 were adopted for the geometry optimization calculations. The energy convergence was set to 2.0×10^{-5} eV. After geometry optimization, the obtained structures were used in the molecular dynamics calculations. One k-point at Γ was used for sampling the Brillouin zone. The molecular dynamics calculation was performed at 300 K to model common experimental conditions. The time step was set to 1 fs, and 5000 steps were calculated. The projected density of states (PDOS) was calculated based on the structure obtained from the molecular dynamics calculations. The adsorption energy (E_{ads}) of the acetic acid and water molecule on the TiO_2 surface was calculated by the following formula:

$$E_{ads} = (E_{slab} + n \times E_{acetic\ acid} + m \times E_{water} - E_{total})/n$$

where E_{slab} is the free energy of the TiO_2 surface; n and m are the number of adsorbed acetic acid molecules and water molecules on the TiO_2 surface, respectively; $E_{aceticacid}$ and E_{water} are the free energy of one acetic acid molecule and one water molecule under vacuum, respectively; and E_{total} is the total free energy of the acetic acid and water molecules adsorbed the TiO_2 surface.

3. Results and discussion

3.1. Effect of water molecule on the adsorption mode of carboxyl groups on TiO_2

We first investigated the adsorption of acetic acid on TiO_2. After dehydrating the TiO_2 at 723 K to remove adsorbed water molecules, 18 μmol (low coverage) and 35 μmol (high coverage) of acetic acid was purged onto the surface of the dry TiO_2. As shown in Fig. 1a, absorptions at 2937 cm^{-1} and 1341 cm^{-1}, which are assigned to the stretching vibration (ν(C—H)) and bending vibration (δ(C—H)) of the methyl group of the acetic acid [17,35,36], are observed for both coverages. The most significant distinctions appear in the vibrations of carboxylate group. At low acetic acid coverage, only the bands at 1540 cm^{-1} and 1451 cm^{-1}, which are attributed to the O—C—O asymmetric and symmetric stretching vibrations (ν(O—C—O)) of acetic acid in the bridged bidentate mode [17,35,36], are observed. At high acetic acid coverage, in addition to the bidentate mode, peaks at 1675 cm^{-1} and 1289 cm^{-1}, attributed to the C═O stretching vibration (ν(C═O)) and the C—O stretching vibration (ν(C—O)) of the carboxyl group, respectively [17,35,36], also appear, indicative of the presence of monodentate-adsorbed acetic acid. However, an absorption for the C═O stretching vibration (ν(C═O)) of molecularly adsorbed acetic acid (at 1710 cm^{-1}) is not observed in either case, suggesting that all

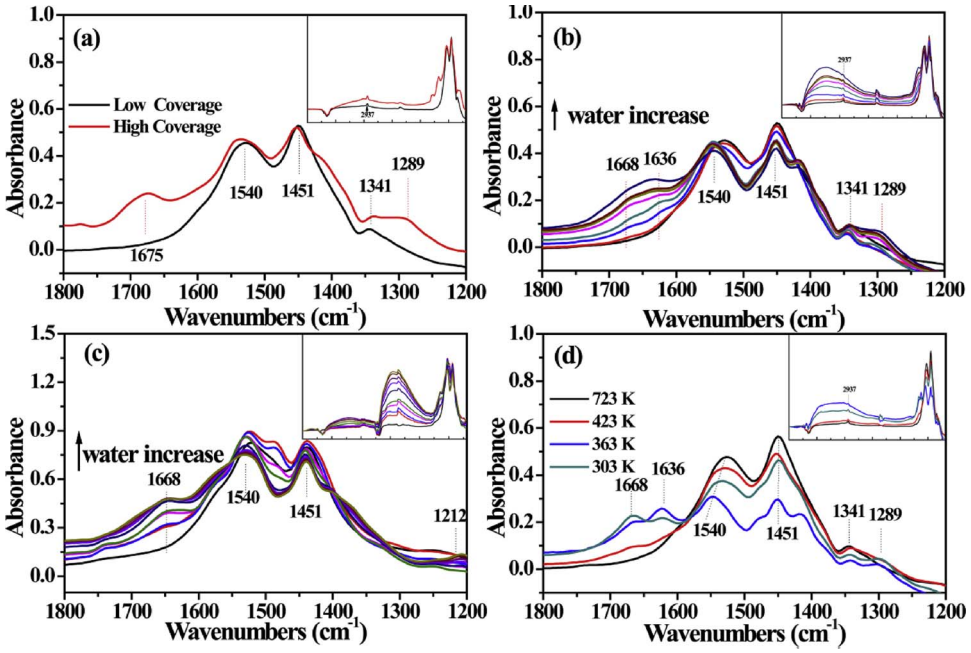

Fig. 1. FTIR spectra of acetic acid/TiO_2 with and without co-adsorbed water. (a) FTIR spectra of dry TiO_2 with different acetic acid coverage; low coverage and high coverage correspond to the samples purged with 18 and 35 μmol of acetic acid vapor, respectively. (b) Spectral evolution of the low-coverage sample while flushing with H_2O vapor and (c) with D_2O vapor. (d) FTIR spectra of TiO_2 with co-adsorbed water/acetic acid after dehydrating at different temperatures. All insets are the corresponding full spectra from 4000 cm^{-1} to 1200 cm^{-1}. All FTIR spectra were collected at 303 K using dry TiO_2 as the background.

the acetic acid is adsorbed on the TiO_2 surface in a coordinative manner under the experimental conditions [17,35,36]. Evidently, at low coverage, acetic acid tends to adsorb in the bidentate bridging mode. The emergence of monodentate-adsorbed acetic acid at high coverage results from the competition for Ti sites when the surface is crowded with acetic acid.

When water molecules were introduced onto the sample with a low coverage of acetic acid, in addition to the IR peaks from water (1636 cm^{-1} for the bending vibrations $\delta(H_2O)$ and 3300 cm^{-1} for the stretching vibrations ν(O—H) of water molecules in a hydrogen-bonding network) [37,27], the peak corresponding to C═O stretching vibrations (ν(C═O) at 1668 cm^{-1}) of monodentate-adsorbed carboxyl was also observed and gradually increased over time. Concomitantly, the intensities of the absorptions from the bidentate-adsorbed carboxyl group (1540 cm^{-1} and 1451 cm^{-1}) decreased (Fig. 1b). We then removed the co-adsorbed water molecules by heating the samples at different temperatures. As shown in Fig. 1d, the intensities of the ν(C═O) (1668 cm^{-1}) and $\delta(H_2O)$ (1636 cm^{-1}) peaks gradually decreased, while the intensities of the ν(O—C—O) absorptions (1540 cm^{-1} and 1451 cm^{-1}) increased. To avoid interference from the IR absorption of the H_2O bending vibration (1636 cm^{-1}) in the measurement of ν(C═O) (1668 cm^{-1}), we examined the effect of co-adsorbed D_2O on the adsorption mode of acetic acid, because the peak corresponding to the D_2O bending vibration is located at 1212 cm^{-1} [37,27]. Similar to H_2O, the addition of D_2O also led to the appearance of the ν(C═O) peak (1668 cm^{-1}) and the decrease in the intensities of the ν(O—C—O) absorptions at 1540 cm^{-1} and 1451 cm^{-1} (Fig. 1c), indicating that co-adsorbed water molecules change the adsorption mode of acetic acid from bidentate to monodentate.

In addition, in spectrum of the co-adsorbed sample, the ν(C═O) peak redshifts from 1675 cm^{-1} (Fig. 1a) to 1668 cm^{-1}, while the $\delta(H_2O)$ absorption blueshifts from 1620 cm^{-1} (on TiO_2 with water adsorption alone; Fig. S2) to 1636 cm^{-1}. Such shifts in the ν(C═O) and $\delta(H_2O)$ IR absorption peaks indicate the existence of hydrogen bonding between the C═O of acetic acid and the co-adsorbed H_2O. We propose that, at low acetic acid coverage, acetic acid is dominantly adsorbed on the surface of TiO_2 in the bridged bidentate mode. The presence of water switches the adsorption mode to monodentate coordination by interacting with the C═O of acetic acid via hydrogen bonding (Scheme 1, also see the theoretical verification in Fig. 7).

3.2. Effect of water on the photocatalytic decarboxylation of the carboxyl group

As mentioned before, only bidentate-adsorbed acetic acid is observed on the dry TiO_2 surface at a low coverage of acetic acid. Under UV irradiation, all the peaks corresponding to acetic acid (1540 cm^{-1} and 1451 cm^{-1} for ν(O—C—O), 2937 cm^{-1} for ν(C—H) and 1337 cm^{-1} for δ(C—H)) gradually decrease concomitantly with an increase in the ν(O—H) peak (3685 cm^{-1}) (Fig. S3a), which is indicative of the degradation of the bidentate acetic acid and the production of water [17,21]. To study the role of water in the photocatalytic decarboxylation of a carboxyl group, water-saturated O_2 was flushed onto the TiO_2 surface with a low coverage of acetic acid. After that, a dehydration process at different temperatures (423 K, 363 K and 303 K) under Ar atmosphere was used to control the amount of water on the surface [38–40]. The sample was then cooled to 303 K under O_2 atmosphere to collect the IR spectrum. In the presence of water, the intensities of the peaks corresponding to the newly formed monodentate acetic acid and bidentate acetic acid significantly decreased under UV irradiation. After 60 min of irradiation, the IR absorption (1668 cm^{-1}) of monodentate acetic acid almost disappears in all the three situations, while the intensities of the peaks corresponding to bidentate acetic acid only decreased slightly (Fig. S3b–d). Moreover, the peak intensities from water molecules, such as those of $\delta(H_2O)$ at 1636 cm^{-1}, ν(O—H) at 3300 cm^{-1} and ν(O—H) at 3685 cm^{-1} from free OH, gradually increased, which is indicative of the formation of water during the oxidation of acetic acid.

To further reveal the effect of water on the photocatalytic oxidation rate of acetic acid, we compared the change in the photoinduced intensities (the deconvolved peak area, as shown in Fig. S4) of ν(C═O) (1668 cm^{-1}, which represents monodentate-adsorbed acetic acid) and ν(O—C—O) (1540 cm^{-1} and 1451 cm^{-1}, corresponding to the bidentate adsorption mode) for the samples dehydrated at different temperatures. As shown in Fig. 2, at all dehydration temperatures, the decay rate of ν(C═O) is much higher than that of ν(O—C—O) (note the difference in the scale of the y-axes). As mentioned above, water is generated during the photocatalytic oxidation of acetic acid (Fig. S3). The resulting water can transform the adsorption mode of acetic acid from bidentate to monodentate. Hence, the faster decrease in monodentate acetic acid is attributed to the faster oxidation kinetics of monodentate acetic acid, rather than the transformation between the two adsorption modes. In

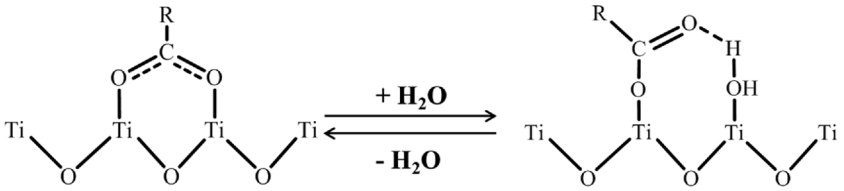

Scheme 1. Switching of the adsorption mode of acetic acid between bridged bidentate coordination to monodentate coordination in the presence of a water molecule.

addition, the decay in the rate constant of ν(C═O) is larger at lower dehydration temperatures, where more water is left on the surface. This observation indicates that in addition to changing bidentate-adsorbed acetic acid to the more easily oxidized monodentate acetic acid, water should have other unknown effects. For example, the co-adsorbed water molecule likely promotes the reaction of O_2 with the photoinduced conduction band electron, which would enhance the overall efficiency by hindering electron-hole recombination.

When H_2O vapor was replaced by D_2O, the degradation of CH_3COOH is not significantly changed, as shown by the decay rate of ν(C═O) in Fig. 3a. Since the cleavage of H—O bond is required for the formation of OH radicals from H_2O, the small kinetic isotope effects (KIEs) suggests that the formation of OH radical is not in the rate-determined step of TiO_2 photocatalytic oxidation of acetic acid. Moreover, the degradation of CD_3COOD in the presence of H_2O also exhibits a similar rate to that of CH_3COOH (KIE ~ 1, Figs. 3 b and S5), suggesting the H-abstraction reaction from the methyl groups (cleavage of the C—H), known to the most possible mechanism for the OH-initiated oxidation of acetic acid, is not in the rate-determined step neither. All these observation do not support the earlier-proposal that the enhancement of water to the photocatalytjc degradation of acetic acid is caused by increased OH radical in the presence of water vapor.

3.3. Effect of water on the adsorption and photocatalytic decarboxylation of trichloroacetic acid (TCA) on TiO_2

To elucidate the origin of the promotive effect of water vapor on photocatalytic decarboxylation, we further examined the role of water on the adsorption and oxidation of TCA, which is known to resist attack from OH radicals. The only oxidative degradation pathway for TCA is direct oxidation by photoinduced holes [41]. As shown in Fig. 4a, when water was introduced onto the TiO_2 sample pre-adsorbed with TCA, an IR peak at 1660 cm^{-1}, assigned to the C═O stretching vibration, emerged and increased in intensity with flushing time, accompanied by the appearance of a shoulder peak at 1636 cm^{-1} from the bending vibration of water. Due to interference from the IR absorption of H_2O bending vibrations (1636 cm^{-1}), the vibration of bidentate-adsorbed O—C—O is difficult to observe. Hence, D_2O was used instead of H_2O, and a similar increase in the intensity of the peak at 1660 cm^{-1} and decrease of peak at 1590 cm^{-1}, assigned to the stretching vibration of bidentate-adsorbed O—C—O, were observed (Fig. 4b). In Fig. 4b, the negative broad peak (3700–2700 cm^{-1}) is observed, resulting from that the D_2O, which has an absorption band ranging from 2500 cm^{-1} to 1800 cm^{-1}, replaces the residual H_2O (3700–2700 cm^{-1}) on the surface, which is inevitable during the pre-adsorbing TCA onto the TiO_2. We also controlled the amount of water by dehydrating the sample at different temperatures. As indicated in Fig. S6, the IR absorbance at 1660 cm^{-1} decreased significantly as the dehydration temperature increased from 303 K to 423 K. We should note that when the dehydration temperature was higher than 500 K, the thermal decomposition of TCA occurred. These observations suggest that, similar to acetic acid, the co-adsorption of water molecules changes the adsorption mode of TCA from bidentate to monodentate.

Under UV irradiation, the bidentate TCA peak (1590 cm^{-1}) for the sample dehydrated at 423 K underwent a larger decrease, and monodentate TCA was expected to be the minor species (Fig. 5a). However, when the sample was dehydrated at 303 K, the absorption at 1660 cm^{-1} (ν(C═O) of monodentate TCA) decreased much more quickly than that at 1590 cm^{-1} (Fig. 5b). These observations suggest that the oxidation rate of monodentate TCA is much quicker than that of bidentate TCA, which is similar to the observations of acetic acid adsorption. Because the only possible pathway for TCA oxidation is decarboxylation via direct oxidation by holes, the faster oxidation of monodentate TCA indicates that this adsorption mode is directly oxidized by photoinduced holes more easily. Hence, our earlier proposal that the promotive effect of H_2O on the photocatalytic decarboxylation of carboxyl compounds results from the enhanced direct oxidation by holes, rather than the enhanced formation of OH radicals as generally believed, is confirmed [17,21].

3.4. Analysis of intermediates during the photocatalytic decarboxylation of acetic acid

When an increased amount of water was introduced into the photoreactor containing 0.1 g of TiO_2 and 18 μmol of acetic acid, the oxidation rate of acetic acid gradually increased (Fig. S7), which is consistent with the IR results. We further analyzed the products from the photocatalytic oxidation of acetic acid on the TiO_2 surface in the presence of co-adsorbed water by GC/MS and GC. The main identified intermediates were methanol, acetone, methane and methyl acetate evidently formed from the esterification of methanol and acetic acid (Fig. S8). The methyl group of the acetic acid remained unchanged in all detected intermediates, which does not support the degradation mechanism of H-abstraction from the methyl group by an OH radical. Rather, the carbon–carbon bond cleavage of acetic acid should dominate the degradation process. The direct oxidation of carboxyl

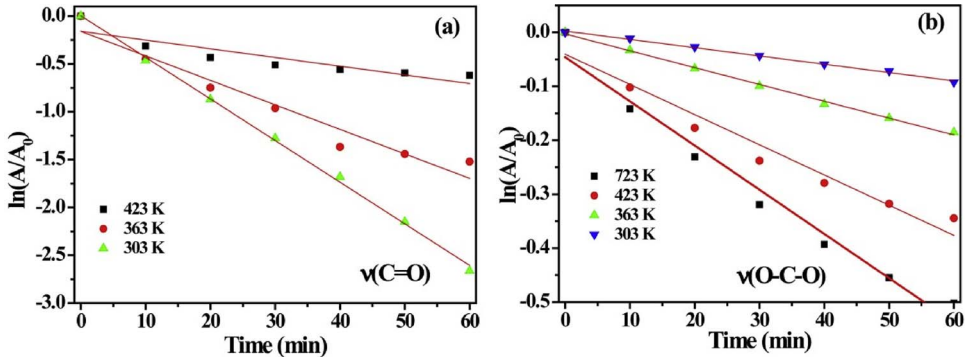

Fig. 2. Effect of the dehydration temperature on the relative peak area ($\ln(A/A_0)$) of (a) ν(C═O) and (b) ν(O—C—O) as a function of irradiation time.

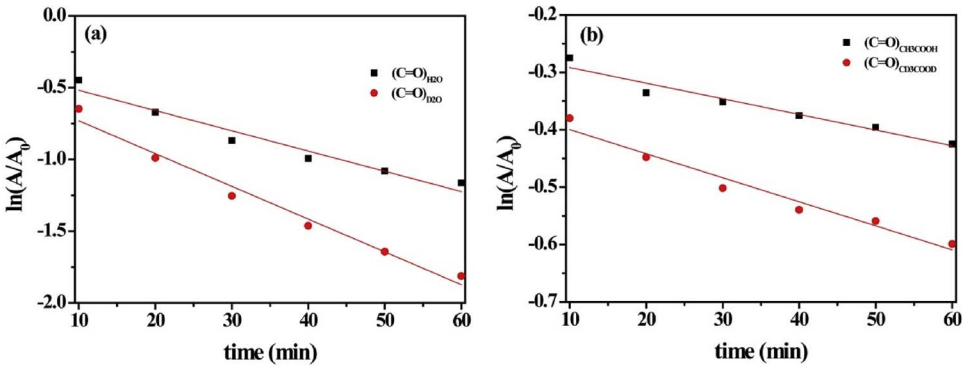

Fig. 3. The relative peak area (ln(A/A0)) of ν(C=O) as a function of irradiation time. (a) The photocatalytical degradation of acetic acid on surface of TiO_2 adsorbed saturated H_2O and D_2O after dehydration at 303 K; (b) the photocatalytical degradation of CH_3COOH and CD_3COOD on surface of TiO_2 adsorbed saturated water after dehydration at 303 K.

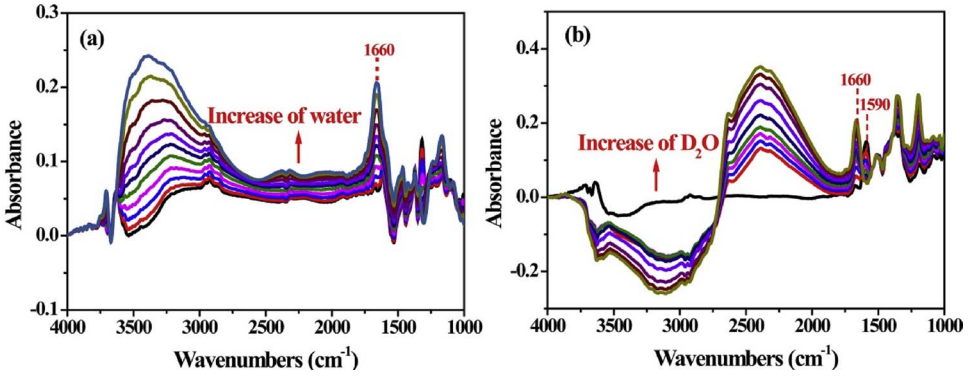

Fig. 4. FTIR spectra collected while flushing the TiO_2 sample pre-adsorbed with TCA with (a) H_2O vapor and (b) D_2O vapor. All FTIR spectra were collected at 303 K using dry TiO_2 as the background.

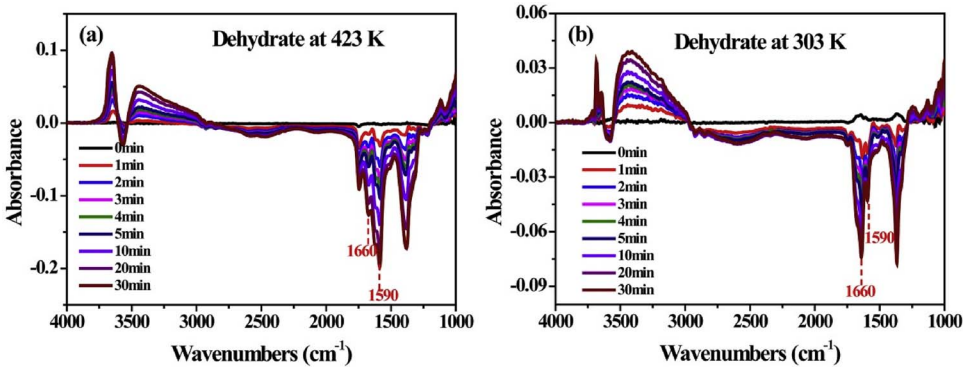

Fig. 5. Time-dependent FTIR spectra of the photocatalytic degradation of TCA on TiO_2 surfaces with saturated adsorbed water after dehydration at (a) 423 K and (b) 303 K. All FTIR spectra were collected at 303 K using samples before irradiation as the background.

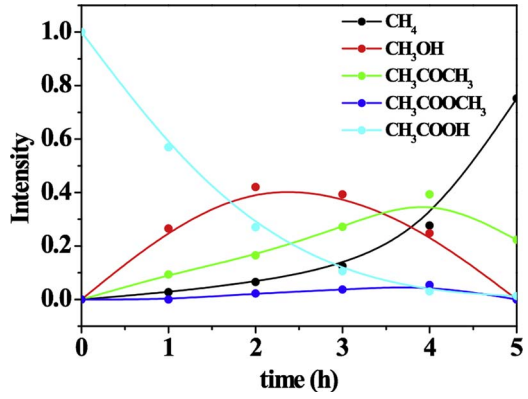

Fig. 6. Time profile of the distribution of intermediates in the photocatalytic oxidation of acetic acid on TiO_2. Conditions: 0.1 g TiO_2, 18 μmol acetic acid and 56 μmol water.

compounds by holes is known to lead to decarboxylation through the cleavage of carbon–carbon bonds through the so-called Kolbe reaction [21,42]. The decarboxylation of acetic acid produces CO_2 and methyl radicals. The reaction between the methyl radical and surface OH or H and the radical coupling reaction can describe the product analysis results well. The distribution of intermediates during irradiation indicates that methanol is the main intermediate in the initial photooxidation step, followed by the formation of acetone, indicating that the formed methanol may take part in the acetone generation reaction (Fig. 6). Methane appears after acetic acid is completely oxidized, suggesting that methane may result from the further reaction of methanol and acetone. As shown in Fig. S7, with an increase in water, the rate of the photocatalytic decarboxylation of acetic acid increased, and the rate of intermediate generation also increased, indicating that water vapor indeed accelerated the decarboxylation of acetic acid via direct oxidation by holes.

3.5. Theoretical calculations

We further simulated the adsorption mode and electronic properties of acetic acid on TiO_2 with and without co-adsorbed water using a DFT-based molecular dynamics method. Because our experiments were typically carried out at low acetic acid coverage, we simulated the adsorption of one acetic acid molecule on a 1 × 3 supercell of the {101}

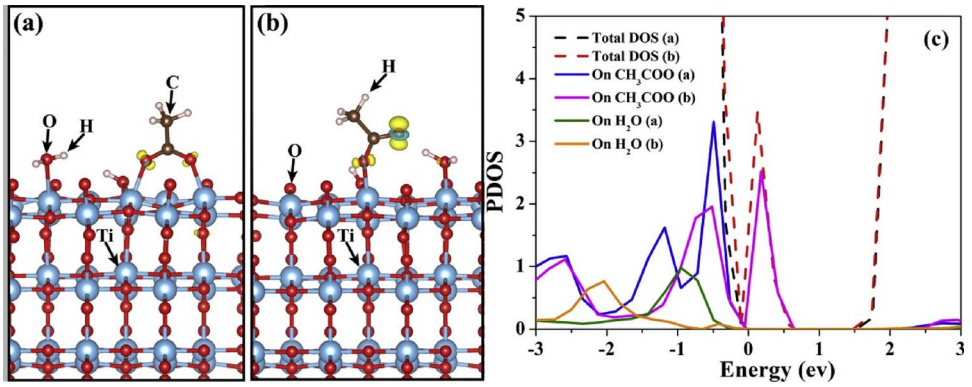

Fig. 7. The influence of co-adsorbed water on the adsorption mode and electronic properties of acetic acid on the {101} surface of TiO_2. (a) To simulate the separate adsorption of water and acetic acid, the water molecule was placed far away from the acetic acid molecule. (b) To show the interaction between the molecules, the water molecule was initially placed near the Ti site at which acetic acid was adsorbed. The *iso*-surfaces in (a) and (b) indicate the spin-density distribution in the presence of one extra hole. (c) The projected density of states (PDOS) of different potential hole trapping sites on the TiO_2 {101} surface. The dashed lines represent the total DOS of the corresponding slabs. All DOS are aligned with the Ti 3 s states in the middle of the slabs.

surface of TiO_2. To simulate the separate adsorption of water and acetic acid, the water molecule was placed far away from the acetic acid molecule (Fig. 7a). Consistent with the aforementioned experimental observations (Fig. 1) and previous theoretical calculations [43], the bridged bidentate adsorption of the acetic acid molecule on the TiO_2 {101} surface is the most stable mode at low coverage in the absence of interactions between the water molecule and acetic acid molecule (Fig. 7a). However, when the water molecule was initially placed near the Ti site at which the acetic acid was adsorbed, the molecular dynamics simulation led to the replacement of the adsorbed O atom of the acetic acid by the water molecule, and the adsorption mode changed from bridged bidentate coordination to monodentate coordination (Fig. 7b). In addition, a hydrogen bond was formed between the O atom of acetic acid and the H atom of water, which is in agreement with our experimental observations of the redshift and blueshift of the stretching vibration absorption of the carbonyl group and the bending vibration absorption of water, respectively, in the presence of water (Fig. 1). The calculated total energy of the co-adsorbed slab is 1.17 eV lower than that of separately adsorbed slab.

To understand the influence of the adsorption mode on the electronic properties, we compared the PDOS of acetic acid in the different adsorption modes, as shown in Fig. 6a and b. First, we aligned the DOS energy level according to the 3 s state of Ti atoms in the middle of the slab. As shown in Fig. S9, the levels of both the conduction band maximum (CBM) and the valence band minimum (VBM) of both slabs are quite similar. However, in the monodentate model, some states exist in the band gap above the VBM. Analysis of the PDOS illustrated that these states originate from acetate, indicating that monodentate acetic acid is easier to oxidize than bidentate acetic acid. Similarly, spin-distribution analysis showed that the spin density of monodentate acetic acid is much larger than that of bidentate acetic acid, when each slab possesses one extra hole. The adsorption of the O atom of acetic acid on the surface Ti sites is achieved by the donation of a portion of the O_{2p} electron to the Ti_{3d} orbital, which leads to a decrease in the electron density on the O atom and thus hinders hole transfer to this O atom. The transformation of bidentate coordination to monodentate coordination upon the co-adsorption of water reduces the amount of electron donation and increases the electron density on the acetic acid. Accordingly, monodentate acetic acid is more easily oxidized by holes. Moreover, in both models, the PDOS of acetic acid is located around the VBM, while the PDOS of the adsorbed water molecules is embedded deeply below the VBM (Fig. 7c). These results suggest that acetic acid more easily traps photoinduced holes than water, and hole transfer from the TiO_2 {101} surface to the adsorbed water molecules to form OH radicals is thermodynamically unfavorable, which is consistent with the above experimental observations in which the photocatalytic oxidation of acetic acid is attributed to direct oxidation by holes, rather than to the attack of OH radicals, even in the presence of water.

4. Conclusions

Our experimental and theoretical results show that water molecules accelerate the photocatalytic decarboxylation by transforming the adsorption mode of carboxyl groups from bidentate to monodentate and that the photocatalytic decarboxylation of monodentate-adsorbed carboxyl groups by photoinduced holes is much quicker than that of bidentate-adsorbed carboxyl groups. This study provides new insights into the effect of water on the photocatalytic decarboxylation of carboxyl compounds on TiO_2. Considering that both carboxyl compounds and water are ubiquitous components of indoor and outdoor air, the present study is useful for developing TiO_2 photocatalysis for the removal of indoor organic pollutants and for the photocatalytic transformation of organic acids in the atmosphere.

Acknowledgements

This work was supported by the 973 project (No. 2013CB632405), the NSFC (Nos. 21590811, 21525729, 21521062), the “Strategic Priority Research Program” of the Chinese Academy of Sciences (No. XDA09030200) and the “CAS Interdisciplinary Innovation Team Program”.

Appendix A. Supplementary data

Supplementary data associated with this article can be found, in the online version, at http://dx.doi.org/10.1016/j.apcatb.2017.10.020.

References

[1] H. Sheng, Q. Li, W. Ma, H. Ji, C. Chen, J. Zhao, Appl. Catal. B: Environ. (2013) 212–218.
[2] N.A. Ab Aziz, P. Palaniandy, H.A. Aziz, I. Dahlan, J. Chem. Res. (2016) 704–712.
[3] P.A.K. Reddy, P.V.L. Reddy, E. Kwon, K.H. Kim, T. Akter, S. Kalagara, Environ. Int. 91 (2016) 94–103.
[4] C. Lai, M.M. Wang, G.M. Zeng, Y.G. Liu, D.L. Huang, C. Zhang, R.Z. Wang, P. Xu, M. Cheng, C. Huang, H.P. Wu, L. Qin, Appl. Surf. Sci. 390 (2016) 368–376.
[5] W. Zou, L. Zhang, L. Liu, X. Wang, J. Sun, S. Wu, Y. Deng, C. Tang, F. Gao, L. Dong, Appl. Catal. B: Environ. 181 (2016) 495–503.
[6] K. Lv, X. Guo, X. Wu, Q. Li, W. Ho, M. Li, H. Ye, D. Du, Appl. Catal. B: Environ. 199 (2016) 405–411.
[7] X. Li, Z. Zhu, Q. Zhao, S. Liu, Appl. Surf. Sci. 257 (2011) 4709–4714.
[8] X. Chen, S.S. Mao, Chem. Rev. 107 (2007) 2891–2959.
[9] J. Arana, A.P. Alonso, J.M. Dona Rodriguez, G. Colon, J.A. Navio, J. Perez Pena, Appl. Catal. B: Environ. 89 (2009) 204–213.
[10] S. Afzal, W.A. Daoud, S.J. Langford, ACS Appl. Mater. Interfaces 5 (2013) 4753–4759.
[11] G. Doganli, B. Yuzer, I. Aydin, T. Gultekin, A.H. Con, H. Selcuk, S. Palamutcu, J. Coat. Technol. Res. 13 (2016) 257–265.
[12] S. Afzal, W.A. Daoud, S.J. Langford, J. Mater. Chem. 22 (2012) 4083–4088.
[13] J. Mo, Y. Zhang, Q. Xu, J.J. Lamson, R. Zhao, Atmos. Environ. 43 (2009) 2229–2246.
[14] M.A. Henderson, J. Catal. 256 (2008) 287–292.
[15] Q. Guo, C.Y. Zhou, Z.B. Ma, Z.F. Ren, H.J. Fan, X.M. Yang, Chem. Soc. Rev. 45 (2016) 3701–3730.
[16] J. Szanyi, J.H. Kwak, J. Mol. Catal. A: Chem. 406 (2015) 213–223.

[17] M. Takeuchi, J. Deguchi, S. Sakai, M. Anpo, Appl. Catal. B: Environ. 96 (2010) 218–223.
[18] L. Ren, M. Mao, Y. Li, L. Lan, Z. Zhang, X. Zhao, Appl. Catal. B: Environ. 198 (2016) 303–310.
[19] A. Fujishima, X. Zhang, D.A. Tryk, Surf. Sci. Rep. 63 (2008) 515–582.
[20] A.D. Belapurkar, V.S. Kamble, G.R. Dey, Mater. Chem. Phys. 123 (2010) 801–805.
[21] K.L. Miller, C.W. Lee, J.L. Falconer, J.W. Medlin, J. Catal. 275 (2010) 294–299.
[22] S. Sato, K. Ueda, Y. Kawasaki, R. Nakamura, J. Phys. Chem. B 106 (2002) 9054–9058.
[23] C. y. Wang, H. Groenzin, M.J. Shultz, J. Am. Chem. Soc. 127 (2005) 9736–9744.
[24] S. Demirci, T. Dikici, M. Yurddaskal, S. Gultekin, M. Toparli, E. Celik, Appl. Surf. Sci. 390 (2016) 591–601.
[25] J.T. Carneiro, C.C. Yang, J.A. Moulijn, G. Mul, J. Catal. 277 (2011) 129–133.
[26] K.L. Miller, J.L. Falconer, J.W. Medlin, J. Catal. 278 (2011) 321–328.
[27] C.E. Nanayakkara, J.K. Dillon, V.H. Grassian, J. Phys. Chem. C 118 (2014) 25487–25495.
[28] P. Zhou, H. Zhang, H. Ji, W. Ma, C. Chen, J. Zhao, Chem. C 53 (2017) 787–790.
[29] G. Kresse, J. Furthmuller, Comput. Mater. 6 (1996) 15–50.
[30] G. Kresse, J. Furthmuller, Phys. Rev. B 54 (1996) 11169–11186.
[31] G. Kresse, J. Hafner, Phys. Rev. B 48 (1993) 13115–13118.
[32] G. Kresse, J. Hafner, Phys. Rev. B 47 (1993) 558–561.
[33] J.P. Perdew, Y. Wang, Phys. Rev. B 45 (1992) 13244–13249.
[34] J.P. Perdew, K. Burke, M. Ernzerhof, Phys. Rev. Lett. 77 (1996) 3865–3868.
[35] A. Mattsson, L. Osterlund, J. Phys. Chem. C 114 (2010) 14121–14132.
[36] J.G. Tao, M. Batzill, J. Phys. Chem. Lett. 1 (2010) 3200–3206.
[37] H. Sheng, H. Zhang, W. Song, H. Ji, W. Ma, C. Chen, J. Zhao, Angew. Chem. Int. Ed. 20 (2015) 5905–5909.
[38] J. Saavedra, H.A. Doan, C.J. Pursell, L.C. Grabow, B.D. Chandler, Science 345 (2014) 1599–1602.
[39] C. Deiana, E. Fois, S. Coluccia, G. Martra, J. Phys. Chem. C 114 (2010) 21531–21538.
[40] W.Q. Fang, X.Q. Gong, H.G. Yang, J. Phys. Chem. Lett. 2 (2011) 725–734.
[41] H. Czili, A. Horvath, Appl. Catal. B: Environ. 89 (2009) 342–348.
[42] B. Wen, Y. Li, C. Chen, W. Ma, J. Zhao, Chem. Eur. J. 16 (2010) 11859–11866.
[43] D.C. Grinter, M. Nicotra, G. Thornton, J. Phys. Chem. C 116 (2012) 11643–11651.